Variability in the distribution of phytoplankton as affected by changes to the main physical parameters in the Baltic Sea*

Lidia Dzierzbicka-Głowacka⋆
Jaromir Jakacki
Maciej Janecki
Artur Nowicki

Institute of Oceanology,
Polish Academy of Sciences,
Powstańców Warszawy 55, Sopot 81–712, Poland;

e-mail: dzierzb@iopan.gda.pl

⋆corresponding author

Abstract

An integrated ecological system model was used to determine the influence on Baltic phytoplankton of the long-term variability in the sea's main physical parameters. A three-dimensional coupled sea-ice model was developed. A simple ecosystem was added to the sea-ice model and used to estimate phytoplankton variability during long-term changes in the main atmospheric forces. Scenarios similar to those of climate were performed by altering the main physical parameters such as temperature, wind speed, solar and thermal radiation (in different configurations). The influence of the variability in these parameters on phytoplankton is discussed.

1. Introduction

The numerous threats and natural disasters elicited by changes in the environment have persuaded experts to radically intensify ecological investigations and forecasts at a regional and global scale. A key part in these changes is played by marine ecosystems, especially the organic matter production processes occurring in them. Marine production is the most important mechanism of carbon exchange between the sea and the atmosphere and therefore requires to be monitored continuously with both traditional methods (from on board ship) and modern remote sensing techniques. This kind of research is extremely expensive and demands the cooperation of interdisciplinary study groups working in laboratories and on board ship. Nevertheless, the effective monitoring of marine production is practically impossible using only traditional methods. During the last four decades, another way of solving these problems has been developed using numerical methods describing the bioproductivity of marine basins. Mathematical models of ecosystems can also be used as tools for forecasting and evaluating the influence of human activities, for analysing future changes in an ecosystem and for visualizing the influence of external factors (Gordon et al. 1995).

The main aim of this work was to study how atmospheric physical parameters (wind speed, air temperature and short-wave radiation) affect the distribution of the phytoplankton biomass in the Baltic Sea. However, the influence of biogeochemical processes, e.g. nutrient concentrations increasing or decreasing through the influx of nutrients from rivers and the atmosphere, on the investigated variables is not considered. This has been examined in another paper (submitted separately, Dzierzbicka-Głowacka et al. 2011).

The 3D Coupled Ecosystem Model of the Baltic Sea was developed at the Institute of Oceanology PAN. It can be used to estimate annual, seasonal, monthly and daily variability in particular parameters, the impact of climatic conditions over several years, and the influence of hydrophysical and biochemical processes on temporal and spatial distributions.

2. The CEMBSv1 model

The CEMBSv1 model is embedded in the existing 3D hydrodynamic model of the Baltic Sea. The POPCICE sea-ice model prescribed in the ECOOP IP WP 10 project (European COastal-shelf sea Operational observing and forecasting system integrated Project) is used to apply biological equations to plankton systems (see Dzierzbicka-Głowacka et al. 2010a for the POC model, Dzierzbicka-Głowacka et al. 2010b for the

copepod model, and here for CEMBSv1). The model employs the Parallel Ocean Program and Community Ice CodE (POPCICE). Both the ocean and the ice models are from the Los Alamos National Laboratory (LANL). POPCICE is forced using European Centre for Medium-Range Weather Forecasts (ECMWF) data: 2-m temperature and dew point, long- and short-wave radiation (downward), 10-m wind speed and air-ocean wind stress. The ocean model time step is 480 s and the ice model time step is 1440 s. The horizontal resolution for the ice and ocean model is ∼9 km (1/12 degree). The vertical resolution (ocean model) is 21 levels (for the Baltic Sea ∼18 levels). The model domain and bathymetry (represented by vertical levels) are presented in Figure 1. There are two images: the left-hand one shows the bathymetry in the model coordinates, the right-hand one the same bathymetry as a geographic projection. The colour scale represents model levels (not depth). In this figure, '3' stands for a maximum depth of 15 m and a cell thickness of 5 m, and '10' means that the maximum depth is ∼80 m and the cell thickness is ∼15 m. Both models operate on the same grid, so there are no problems with exchanging fluxes between them. In this paper, however, we focus only on the biological part of the 3D model.
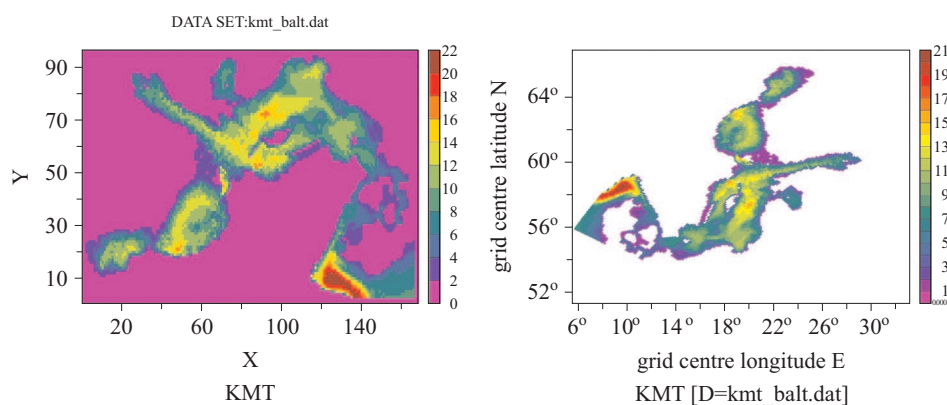

Figure 1. Model domain and bathymetry (model coordinates – left-hand side, stereographic coordinates – right-hand side)

2.1. Conceptual basis

The 3D ecosystem model is based on the 1D biological model of Dzierzbicka-Głowacka (2005, 2006). In this model, phytoplankton is represented by one state variable, and the model formulations are based on the simple total inorganic nitrogen ($NO_3 + NO_2 + NH_4$) cycle. Initially, this nutrient serves to trigger the phytoplankton bloom but later to limit

phytoplankton production. The set of CEMBSv1 equations with the biogeochemical processes and parameter values are given in Appendix A and Table 1.

Table 1. Parameterization of the 3D CEMBSv1 model

F_S	Mathematical formulation
primary production	$PRP = f_{\max} f_I f_N Phyt$
	$f_I = \dfrac{I_{PAR}}{I_{\mathrm{opt}}} \exp\left(1 - \dfrac{I_{PAR}}{I_{\mathrm{opt}}}\right)$
	$I_{PAR} = I_o \exp(-k\,z)$, $k = 0.17 + 25(Phyt \times 10^{-3}/\mathrm{g_{Chl}})$, $\mathrm{g_{Chl}} = \mathrm{gC/gChl} = 50/1$, $I_{\mathrm{opt}} = 60$ W m^{-2}, $f_{max} = 1.5$ day^{-1}
	$f_N = \dfrac{NutrN}{K_N + NutrN}$, $K_N = 0.18$ mmolN m^{-3}
zooplankton grazing	$GRZ = g_{\max} \dfrac{Phyt - Phyt_o}{k_{Phyt} + Phyt - Phyt_o} Zoop$
	$g_{\max} = 0.3$ day^{-1}, $k_{Phyt} = 100$ mgC m^{-3}, $Phyt_o = 10$ mgC m^{-3}
mortality of phytoplankton	$MORP = mp\,Phyt$, $mp = 0.05$ day^{-1}
respiration of phytoplankton	$RESP = f_{\max}(r_{PR} f_I f_N + r_{BR}) f_T Phyt$
	$r_{PR} = 0.05$, $r_{BR} = 0.1$, $f_T = \exp(0.0769(T - 10))$
faecal pellets	$FEC = fGRZ$
excretion of zooplankton	$EXCZ = ez\,GRZ$
mortality of zooplankton	$MORZ = mz\,GRZ$, $f = 0.33$, $ez = 0.33$, $mz = 0.33$
predation by other zooplankton	$PRED = p_{\max} \dfrac{Zoop}{k_z + Zoop} Zoop$
	$p_{\max} = 0.1$ day^{-1}, $k_z = 1$ mgC m^{-3}
phytoplankton uptake	$UPT = PRP - RESP_{\mathrm{light}}$
release	$RELE = RESP_{\mathrm{dark}}$
benthic regeneration	$REGD = g_N\,r_D\,Detr$, $g_N = 0.013$ (mmolN (mgC)$^{-1}$)

The model is conceived for a typical shallow sea, the mixed layer being replenished with nutrients from the bottom. The water column dynamics is implemented in a three-dimensional frame, where phytoplankton and nutrient (nitrogen) are transported by advection and diffusion. The physical framework, including all the necessary forcing, is presented in Figure 2.
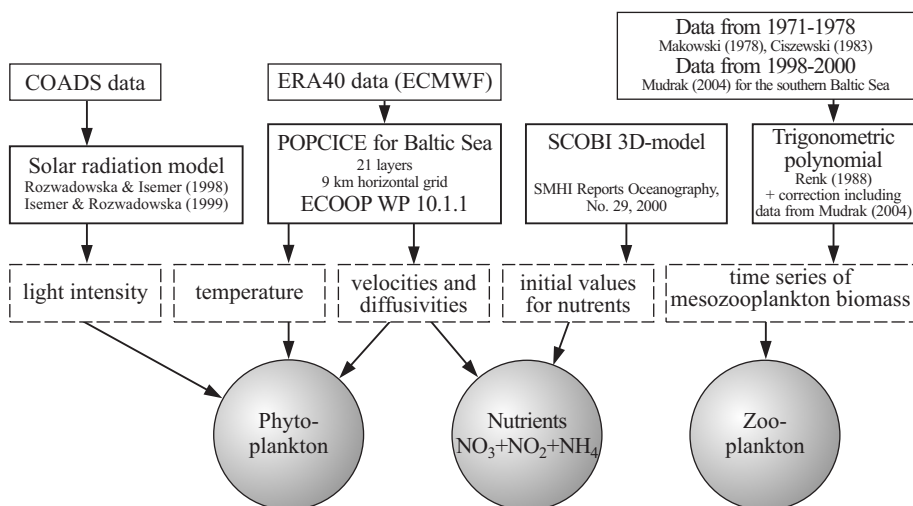

Figure 2. Diagram showing the forcing data and related state variables in the model

The biological model incorporates formulations for the primary production and remineralization mechanisms in the mixed layer, in the lower layer and at the bottom. Primary producers are transported, die and are consumed by zooplankton (mesozooplankton). The grazed phytoplankton is divided into three parts: one contributes to zooplankton growth, another is deposited as faecal pellets, and the third is excreted by zooplankton as dissolved metabolites; thus, it replenishes the nutrient pool. A proportion of the material contributing to growth is assumed to be lost immediately – this represents dying zooplankton. Proportions of both faecal and excreted material are immediately regenerated (Radach & Moll 1993, Dzierzbicka-Głowacka 2005). Phytoplankton mortality is modelled in two ways: a) grazing by mesozooplankton, which form the bulk of the grazers in the Baltic Sea – here it is described by the mesozooplankton biomass; b) all other kinds of mortality, like cell lysis and grazing by zooplankton other than mesozooplankton, are assumed to be proportional to the phytoplankton standing stock, with a constant mortality rate, and therefore dynamically coupled to the phytoplankton dynamics.

The assumed time scale for the sinking of faecal and dead material a few days old (Jickells et al. 1991) is much less than the time scale for benthic regeneration processes, which is from weeks to months (Billen et al. 1991). Therefore, most of the detrital material is deposited on the bottom, where it collects as a benthic pool. Only a small portion of detritus remains suspended in the water column (Postma & Rommets 1984), i.e. 20% of the remineralized dead phyto- and zooplankton and faecal material in the water column. The effect of the microbial food web (Azam et al. 1983) is parameterized by converting this portion of detrital material immediately into regenerated nutrients in the water column. The major portion is deposited on the bottom, where it is re-worked by benthic communities. The concept of a bottom detrital pool has been introduced to create a lag in the remineralization of the majority of detritus and the eventual replenishment of the upper layer with nutrients. This complex process is parameterized by assuming a net remineralization rate for bottom detritus (Billen et al. 1991). Thus, there are two pathways for the regeneration of pelagic and benthic nutrients, each with a different time scale. The availability of regenerated nutrients for production in the upper layers is controlled by physical processes and depth.

Benthic detritus varies according to the input of detrital material from the water column and losses by remineralization. Small biogenic particles, such as individual phytoplankton cells, sink very slowly (< 1 m day^{-1}), and through various aggregation processes, small particles are repacked into larger detrital particles that fall rapidly with sinking velocities of 10–100 m day^{-1} (see Radach & Moll 1993). In shallow seas like the Baltic, biogenic particles have a greater probability of reaching the sediments with much of their organic matter intact than in deep water. In a similar way, zooplankton faecal material is added to the benthic detritus, and nutrients are returned to the water column after remineralization.

Since the intention here is to make the model as simple as possible, and also to avoid having to include several nutrient components, the model is based on total inorganic nitrogen. This is the main factor controlling the biomass of phytoplankton in the Baltic Sea (Shaffer 1987), although cyanobacteria overcome N shortage by N-fixation, so primary production is actually limited by available phosphorus.

In this model, phytoplankton is modelled with the aid of only one state variable represented by diatoms. Cyanobacteria blooms are not incorporated at this stage of the model development. This means that nutrients can be represented by one component – total inorganic nitrogen (Shaffer 1987).

2.2. Equations

Two partial differential equations describe spatial and temporal evolution in total inorganic nitrogen $Nutr(x, y, z, t)$ [mmolN m^{-3}] and phytoplankton $Phyt(x, y, z, t)$ [mgC m^{-3}] pools, and an ordinary differential equation describes the benthic detritus $Detr(x, y, t)$ [mgC m^{-2}] pool. The set of equations with model parameters is given in Appendix A.

The first four terms on the right-hand side of the phytoplankton equation describe the horizontal and vertical advection and diffusion of phytoplankton, where u, v and w are the time-dependent velocities obtained from our model for the Baltic Sea (POPCICE, see ECOOP WP 10.1.1), K_x, K_y, K_z are the horizontal and vertical diffusion coefficients, PRP is gross primary production, $RESP$ is respiration, $MORP$ is mortality and GRZ is grazing. Gross primary production (PRP) is calculated from the nutrient and light limitation functions f_N and f_I. Steele's function (Steele 1962) with optimal light intensity I_{opt} is used as a light limitation function which includes photoinhibition.

For nutrient limitation the Michaelis-Menten formula is applied with constant K_N as the half-saturation constant. Respiration ($RESP$) consists of basal maintenance and photorespiration, each being proportional to the phytoplankton biomass, where the basic dark respiration r_{BR} is proportional to the maximum photosynthetic rate, and the photorespiration r_{PR} is proportional to the gross primary production. The temperature dependence f_T is modelled according to $f_T = \exp(0.0769(T - 10))$, with the constant 0.0769 expressing the respiration change f_T with temperature: it doubles for every 10°C increase in temperature, so that $f_T(T_o) = 1$ at $T_o = 10$°C. Phytoplankton mortality ($MORP$) is assumed to be proportional to the phytoplankton standing stock, with a mortality rate mp. Copepod grazing (GRZ) is assumed to be proportional to the copepod biomass $Zoop$ with rate g_{max}, but this rate is modified by the Michaelis-Menten function of phytoplankton biomass with the half-saturation constant k_{Phyt} subject to a threshold $Phyt_o$, below which grazing ceases.

The state equation for nutrients includes the first four terms on the right-hand side expressing the horizontal and vertical advection and diffusion of nutrients, where the same velocities and diffusion coefficients are used as for phytoplankton, and the four processes are nutrient uptake (UPT), dark respiratory release ($RELE$), remineralization in the water column (REM) and zooplankton excretion ($EXCZ$). Nutrient uptake (UPT) appears in the nitrogen equation for positive net production only in the euphotic zone. The constant g_N is the N:C ratio according to the Redfield ratio. Respiration in the dark consumes particulate organic matter. To conserve matter, the respiration term in the equation for

phytoplankton carbon must be balanced by a nutrient release term ($RELE$) in the equation for nitrogen. This term parameterizes the contribution of respiration to the nutrient pool at the given fixed ratio g_N. For light intensities below the compensation intensity, the respiratory release is regenerated immediately into nitrogen. The fractions of dead phyto- and zooplankton and of faecal pellets that are instantaneously remineralized in the water column by the microbial food web (REM) are given by the proportionality factors p_M for phytoplankton, p_Z for zooplankton and p_F for faecal pellets. Excretion of dissolved ($EXCZ$) and particulate material is parameterized as fixed proportions of zooplankton grazing (ez), faecal pellet production (f) and zooplankton mortality (mz), on condition that $ez + f + mz = 1$.

The benthic detritus equation consists of two terms: sedimentation out of the water column to the bottom (indicated by the integration from the surface to the bottom H, simultaneously from all depths), and regeneration at the bottom. The effect of sedimentation of detrital material out of the water column consists of the contributions by dead phytoplankton, faecal pellets and dead zooplankton, which are not remineralized in the water column by the microbial food web. Remineralization at the bottom is assumed to be proportional to the amount of available benthic detritus, at a constant rate r_D.

2.3. Parameters

The set of constants is given in Appendix A. There now follow a few remarks regarding their choice. For the grazing formulation, the threshold value $Phyt_o$ and the half-saturation value k_{Phyt} have been changed according to data reported by Dzierzbicka-Głowacka (2005). The nitrogen to carbon ratio g_N is assumed to be 0.013 mmolN $(\text{mgC})^{-1}$, the half-saturation constant for total inorganic nitrogen is 0.5 mmolN m^{-3}, and the optimal light intensity for the phytoplankton community is set at 60 W m^{-2}.

For the remineralization rates in the water and at the bottom (following Postma & Rommets (1984)) ca 20% of the average labile particulate organic carbon (POC) is mineralized daily. Thus, 20% of the POC formed as detritus is remineralized instantaneously ($p_F = p_M = p_Z = 0.2$), whereas the remaining 80% is transported immediately to the bottom. There is no explicit sinking of living phytoplankton, because this is already included in the instantaneous transfer to the bottom (Figure 2). Ingested material is divided equally between dead zooplankton, faecal pellets and soluble excretion following Steele (1974). The benthic nutrient mineralization r_D is taken to be 0.0005 day^{-1} exp(0.005°C^{-1} T) (Savchuk & Wulff 1996).

2.4. Forcing

The intention was to simulate production in a physical environment that would be as realistic as possible. Actual oceanic forces are required for reliable simulations of phytoplankton dynamics (Figure 2). The external forcing is taken from ECMWF (ERA 40 reanalysis, www.ecmwf.int). The biological reaction terms are not implemented in the circulation model. The primary production model is an independent transport model that uses the circulation model output, so there is no feedback from the biology to the physics, which makes the simulations easier to implement.

Another important force for primary production simulations is solar radiation with its own daily cycle. The total irradiance at the surface is calculated using the model by Rozwadowska & Isemer (1999). The local weather conditions were recorded on board Voluntary Observing Ships, and these data have been used to estimate the climatological characteristics of the solar radiation flux at the sea surface. The monthly loads were interpolated to give daily values.

Nutrient contributions from rivers are not included in this model, but the initial values for nutrients have been based on the SCOBI 3D-model.

Phytoplankton production is limited in the model by light and total inorganic nitrogen. The phytoplankton biomass is restricted by mesozoo-plankton grazing. The zooplankton biomass is prescribed as a force and the model uses the abundance data from Mańkowski (1978), Ciszewski (1983) and Mudrak (2004) for the southern Baltic Sea. Using these observed biomass values and abundances, the annual cycles of abundances are converted to carbon biomass cycles. A trigonometric polynomial is used to assign values at any model time and for all of the grid points.

2.5. Initial and boundary values

Initial phytoplankton values for January and December are very limited, so a constant value of 0.1 mgC m^{-3} is defined; but the model is not sensitive to the initial conditions of phytoplankton concentration (in January). Also, the data for the detritus content at the bottom are not available, so the instantaneous sinking of detritus is a more arbitrary model assumption. The initial amount of detritus at the bottom is prescribed as 200 mgC m^{-2} for the whole Baltic Sea. The initial values for total inorganic nitrogen are taken from SCOBI 3D-model for January.

The initial vertical distributions of nutrient, phytoplankton, zooplankton and detritus pool are known:

$$\{Phyt\}(x,y,z,0) = \{Phyt\}_0(x,y,z) \quad 0 \leq z \leq H,$$
$$\{Nutr\}(x,y,z,0) = \{Nutr\}_0(x,y,z) \quad 0 \leq z \leq H,$$

$$\{Detr\}(x, y, H, 0) = \{Detr\}_0(x, y, H) \quad z = H.$$

The vertical gradients of the phytoplankton and nutrient concentration fluxes are zero at the sea surface ($z = 0$):

$$F_{Phyt}(x, y, 0, t) \equiv K_z \frac{\partial \{Phyt\}(x, y, z, t)}{\partial z}\bigg|_{z=0} - w_z\{Phyt\}(x, y, 0, t) = 0,$$

$$F_{Nutr}(x, y, 0, t) \equiv K_z \frac{\partial \{Nutr\}(z, t)}{\partial z}\bigg|_{z=0} = 0.$$

The bottom flux condition for phytoplankton and nutrient is given by

$$F_{Phyt}(x, y, H, t) \equiv -w_z\{Phyt\}(x, y, H, t),$$

$$F_{Nutr}(x, y, H, t) \equiv K_z \frac{\partial \{Nutr\}(x, y, z, t)}{\partial z}\bigg|_{z=H} = g_N REMD.$$

This flux $F_{phyt}(H)$ enters the benthic detritus equation as a source term. The boundary condition provides the mechanism by which the water column is replenished by nutrients derived from benthic remineralization.

3. Comparison of model results with measurements

In order to assess the accuracy of the CEMBSv1 model for determining the parameters of the Baltic ecosystem, we compared the temperatures and chlorophyll a concentrations obtained from the model with those measured in situ and in water samples for five years (2000–2004). For these comparisons the relevant errors of these simulations were calculated in accordance with the principles of arithmetic and logarithmic statistics:

1. Arithmetic statistics:	2. Logarithmic statistics:
a) Relative mean error: $< \varepsilon >$ [%] (systematic)	e) Mean logarithmic error: $< \varepsilon >_g$ [%] (systematic)
$< \varepsilon > = \frac{1}{N} \sum_i \varepsilon_i$	$< \varepsilon >_g = 10^{<L>} - 1$
where	where
$\varepsilon_i = x_{i,\,mod} - x_{i,\,exp}/x_{i,\,exp}$	$L = \log(x_{i,\,mod}/x_{i,\,exp})$
b) Standard deviation of ε: σ_ε [%]	f) Standard error factor: χ
$\sigma_\varepsilon = \sqrt{\frac{1}{N}\left(\sum_i (\varepsilon_i - < \varepsilon >)^2\right)}$	$\chi = 10^{\sigma_L}$ where σ_L is standard deviation of L

c) Absolute mean error:

$< \varepsilon' >$ [%]

$< \varepsilon' > = \frac{1}{N} \sum_i \varepsilon'_i$

where $\varepsilon'_i = x_{i,\text{mod}} - x_{i,\text{exp}}$

d) Standard deviation of ε':

$\sigma_{\varepsilon'}$ [%]

$\sigma_{\varepsilon'} = \sqrt{\frac{1}{N} \left(\sum_i (\varepsilon'_i - < \varepsilon' >)^2 \right)}$

g) Statistical logarithmic errors:

σ_-, σ_+ [%]

$\sigma_- = 1/\chi - 1$

$\sigma_+ = \chi - 1$

where $x_{i,\text{mod}}$ – calculated values, $x_{i,\text{exp}}$ – measured values.

The following aspects were taken into account in the assessment of the modelled ecosystem parameters:

1. for the sea surface temperature – the relevant absolute errors determined by arithmetic statistics;

2. for the surface concentration of chlorophyll a – the relevant relative errors determined by both arithmetic and logarithmic statistics.

Figure 3 and Table 2 present the results of the validation of the model for sea surface temperature. The figure compares the modelled values of this temperature (T_{mod} – the value from the first layer – 5 m) with values measured in situ (T_{exp} – the mean value from the 0–5 m layer) at particular
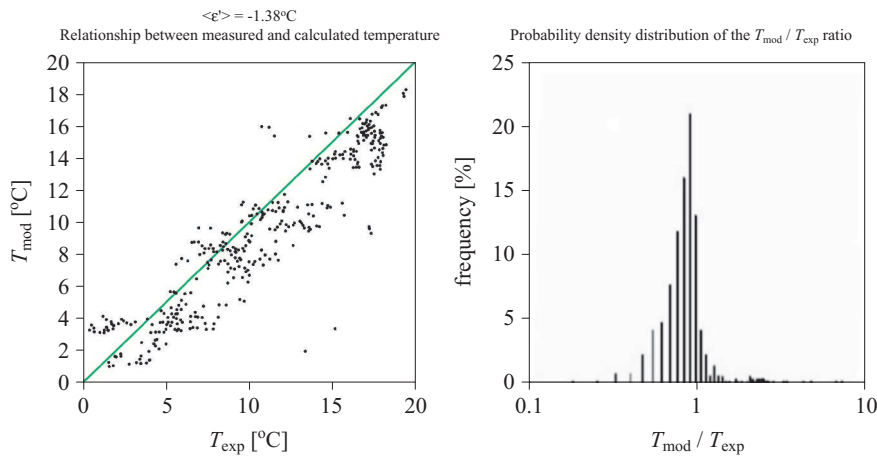

Figure 3. Comparison of measured (T_{exp}) and calculated (T_{mod}) sea surface temperatures from the CEMBS1 model: a) relationship between measured and calculated temperatures; b) probability density distribution of the ratio of the modelled T_{mod} to T_{exp} measured in situ

Table 2. Relative errors in estimating the sea surface temperature from the CEMBS1 model

Arithmetic statistic	
systematic error $< \varepsilon' >$ [°C]	statistical error $\sigma\varepsilon'$ [°C]
−1.38	0.046

measurement stations. The calculated errors (systematic and statistical) in the southern Baltic Sea are ca 1.4°C and 0.05°C. As far as diagnosing the state of the Baltic ecosystem is concerned, this level of accuracy is satisfactory, because the model state parameters are calculated for the whole cell (an area of 9×9 km^2) and not for the particular points at sea where the in situ measurements were made.

The discrepancy for low temperatures (< 5°C) between modelled and observed data (January, February) is probably due to the influence of wind speed changes. These have no substantial effect on the phytoplankton biomass distribution during winter because the growing season begins in March and ends in December, when the temperature is > 5°C. The minimal differences between the modelled and observed results yield larger errors for lower than for higher values, a factor that should be taken into consideration.

The analysis of the modelled surface concentration of chlorophyll a CH_{mod} (value for the first 5 m layer) was carried out jointly for the entire experimental material, i.e. for 196 points from the southern Baltic Sea (measurement data available from IO PAN). Validation was performed in order to estimate the errors for all the data in the empirical data sets. The results of the error analysis are presented in Figure 4 and Table 3. There are several reasons for these errors. One is that the CEMBS1 model only accounts for a fixed C:Chl a ratio of 50:1. In reality, the biomass during the secondary bloom is usually high, whereas the chlorophyll content in the cells is low. To fully take into account this effect, a variable C:Chl a ratio should be included in the model. Another reason is that in this 3D model, phytoplankton is represented by one state variable and the model formulations are based on the simple total inorganic nitrogen ($NO_3 + NO_2 + NH_4$) cycle. A third reason is that the model calculates the surface concentration of chlorophyll a of a whole pixel (an area of 9×9 km^2) and not that of the particular point at sea where the in situ measurement was made. This effect is reduced by increasing the horizontal and vertical resolution; this will be the next obvious step in development of this model, in addition to improving the mixing parameterization.
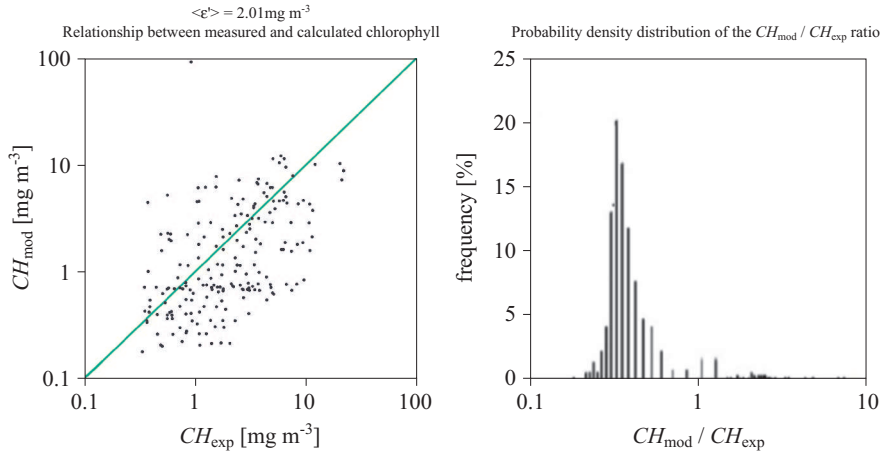
Figure 4. Comparison of surface chlorophyll a concentrations measured (CH_{exp}) and determined from the CEMBS1 model (CH_{mod}): a) relationship between surface chlorophyll a concentrations measured (mean values from the 0–5 m layer) and determined from the CEMBS1 model (values from the first layer); b) probability density distribution of the ratio of the modelled CH_{mod} to the CH_{exp} measured in situ

Table 3. Relative errors in estimating the surface chlorophyll a concentration on the basis of modelled data from the CEMBS1 model

Arithmetic statistic		Logarithmic statistics			
systematic error	statistical error	systematic error	standard error factor	statistical error	
$< \varepsilon >$ [%]	$\sigma\varepsilon$ [%]	$< \varepsilon >$g [%]	χ	$\sigma-$ [%]	$\sigma+$ [%]
-12.88	7.55	83.06	2.53	-60.39	152.5

The consequences of primary production parameterization without the inclusion of cyanobacteria are most likely the lower phytoplankton biomass in the simulations in the spring bloom and the discrepancies between the low simulated and high observed chlorophyll concentrations during summer. The temporal and spatial variabilities in zooplankton distribution throughout the Baltic Sea, not obtained in this model, may also explain the differences between modelled and measured values. The spatial differences between simulated and observed results and their temporal variability in the seasonal cycle are quite similar in each grid box.

We believe that despite these discrepancies, this 3D CEMBS version 1 can be used to assess any increase or decrease in phytoplankton biomass in the next few years as a result of the influence of selected meteorological components on the investigated variables.

4. Results and discussion

The calculations were carried out assuming the following three scenarios following the ECOOP Project [ECOOP Annual Report Part I p. 141, http://www.ecoop.eu/ecoop_docs.php]:

1) a 3° increase in air temperature;

2) a 3° increase in air temperature, a 30% increase in wind speed and a 20% increase in short-wave radiation;

3) a 3° increase in air temperature, a 30% increase in wind speed and a 20% decrease in short-wave radiation.

All the scenarios are based on A1B IPCC (Intergovernmental Panel on Climate Change) climate scenarios. They assume an average emission of CO_2, where the two extreme scenarios were averaged (A1 – mostly pessimistic and B1 – mostly optimistic, http://www.ipcc-data.org/ddc_co2.html).

Daily, biweekly, monthly, seasonal and annual variabilities of the investigated variables were calculated for 45 years (scenarios 1, 2 and 3).

The starting-point of the numerical simulations was assumed to be the end of 2004 and was followed by the repetition of all ERA40 years. The three scenarios were performed for the repeated forcing data.

We chose nine locations within our domain to present phytoplankton biomasses. These stations are: the Gulf of Gdańsk, Gdańsk Deep, Gotland Deep, Bornholm Deep, Gulf of Finland, Gulf of Riga, Gulf of Bothnia, Bothnian Sea and Danish Straits (see Figure 5).

Biogeochemical processes in large areas are strongly dependent on the hydrodynamics of the sea, which in turn are driven meteorologically.

Based on these scenarios, the long-term variabilities of temperature, phytoplankton and nutrients in different areas of the Baltic Sea are calculated for 45 years.

For the proper operation of the model in the coming years, the relationships between phytoplankton biomass and nutrient concentrations (Figure 6a) and also temperature (Figure 6b) are shown for all nine locations. According to the findings for scenario 1, the distributions of points representing these connections are in agreement with reality; for scenarios 2 and 3, the distributions are very similar.

In accordance with phytoplankton biomass dynamics (Figures 6a, b), the season begins with high total inorganic nitrogen concentrations and a low phytoplankton biomass in the 0–4°C range in the whole Baltic Sea (1). When the spring bloom starts at ca 4°C, nutrients are consumed, the total inorganic nitrogen concentrations become low (2), and the bloom is maintained by the external supply of nutrients. In summer (June–August),
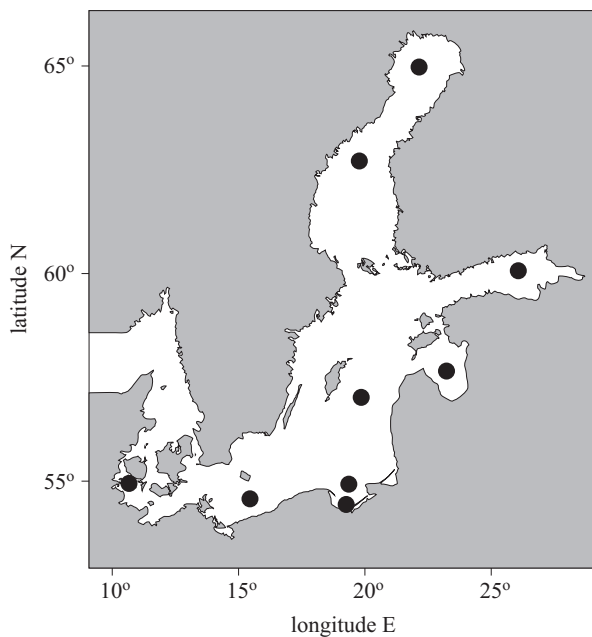
Figure 5. Locations of the stations

1 - winter   2 - spring bloom   3 - summer   4 - autumn bloom
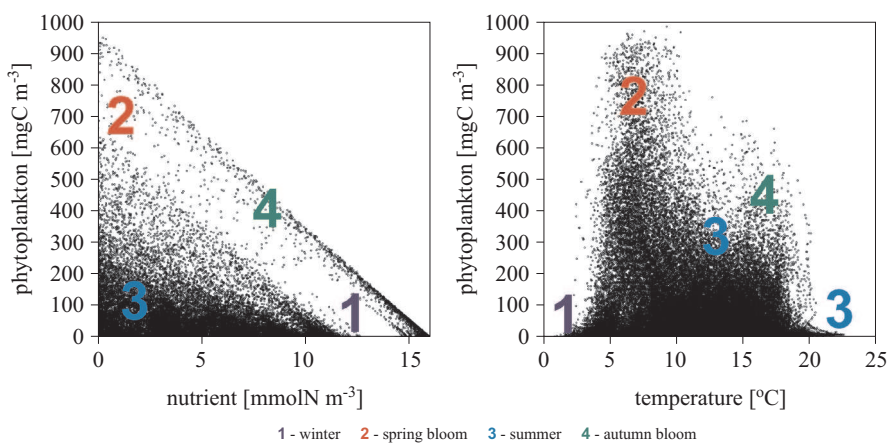
Figure 6. Relation between phytoplankton biomass and nutrient concentrations
(a) and temperature (b) for the nine stations

the phytoplankton biomass is low (3) as a result of the faster depletion of
nutrients.

In the second part of the year, in September and October, there is
a slight rise in the phytoplankton biomass (4) caused by the increase in
nutrient concentrations resulting from the deeper mixing of the water. The

growing season ends in December, when the phytoplankton biomass drops to the January–February level (1).

Taking into account the assumptions given earlier for the three scenarios, the shapes of the one-year distributions of the maximum sea surface temperature $T_{\max}$ at selected stations are the same in all the scenarios; this means that the maximum and minimum temperatures appear at the same times. The calculations also show that the differences in $T_{\max}$ between scenarios 1, 2 and 3 for the first 20 years are insignificant and that the distributions of $T_{\max}$ are very similar in each scenario. In the first scenario, there is a small average increase (ca 0.8°C) of $T_{\max}$ in the whole Baltic Sea for the period investigated. Case 2 predicts an increase in $T_{\max}$ from 22.08°C (in the first year) to 24.12°C (after 45 years), whereas case 3 envisages a decrease of $T_{\max}$ to 19.91°C (after 45 years). The difference in $T_{\max}$ between these cases is ca 2°C. Compared to case 1, the respective increase and decrease in $T_{\max}$ is ca 1.3°C and 3°C in cases 2 and 3. This is due to the influence of short-wave radiation, which compensates for changes in temperature. Moreover, the increasing wind speed and westerly component of the wind speed mean that the drop in $T_{\max}$ in case 3 is greater than the rise forecast by case 2 (a respective 20% decrease and increase in short-wave radiation).

Time series of the one-year averaged $Phyt_{\mathrm{ave}}$ and annual maximum $Phyt_{\max}$ of the phytoplankton biomass at the nine stations are shown in Figures 7 and 8. Comparison of $Phyt_{\mathrm{ave}}$ and $Phyt_{\max}$ of the phytoplankton biomass in the subsurface layer shows that there are only slight differences between these parameters foreseen by scenarios 2 and 3. This implies that short-wave radiation has a negligible influence on the distribution of phytoplankton biomass. In addition, the results indicate that the distributions of $Phyt_{\mathrm{ave}}$ and $Phyt_{\max}$ for the three scenarios differ little in the gulfs (Gdańsk, Finland, Riga and Bothnia). In the other regions investigated (Gdańsk Deep, Gotland Deep, Bornholm Deep, Bothnia Sea and Danish Straits), however, there are evident differences in $Phyt_{\mathrm{ave}}$ and $Phyt_{\max}$ between scenarios 1 and 2/3: they are higher in cases 2 and 3 than in case 1, i.e. $Phyt_{\mathrm{ave}}$ is ca 10 mgC m^{-3}, $Phyt_{\max}$ from 100 to 250 mgC m^{-3}. This corresponds to the depths of these regions: $Phyt_{\max}$ increases by 20% (ca 100 mgC m^{-3}) in the Bornholm Deep and by 50% (ca 250 mgC m^{-3}) in the Gotland Deep.

The results show significant changes in the distributions of phytoplankton biomass $Phyt$ in open sea areas, where there is a considerable increase in current velocities. Scenarios 2 and 3 predict increased turbulence (mixing) (30% faster wind speed and westerly wind speed component), and hence an increase in phytoplankton biomass distributions. This is the result
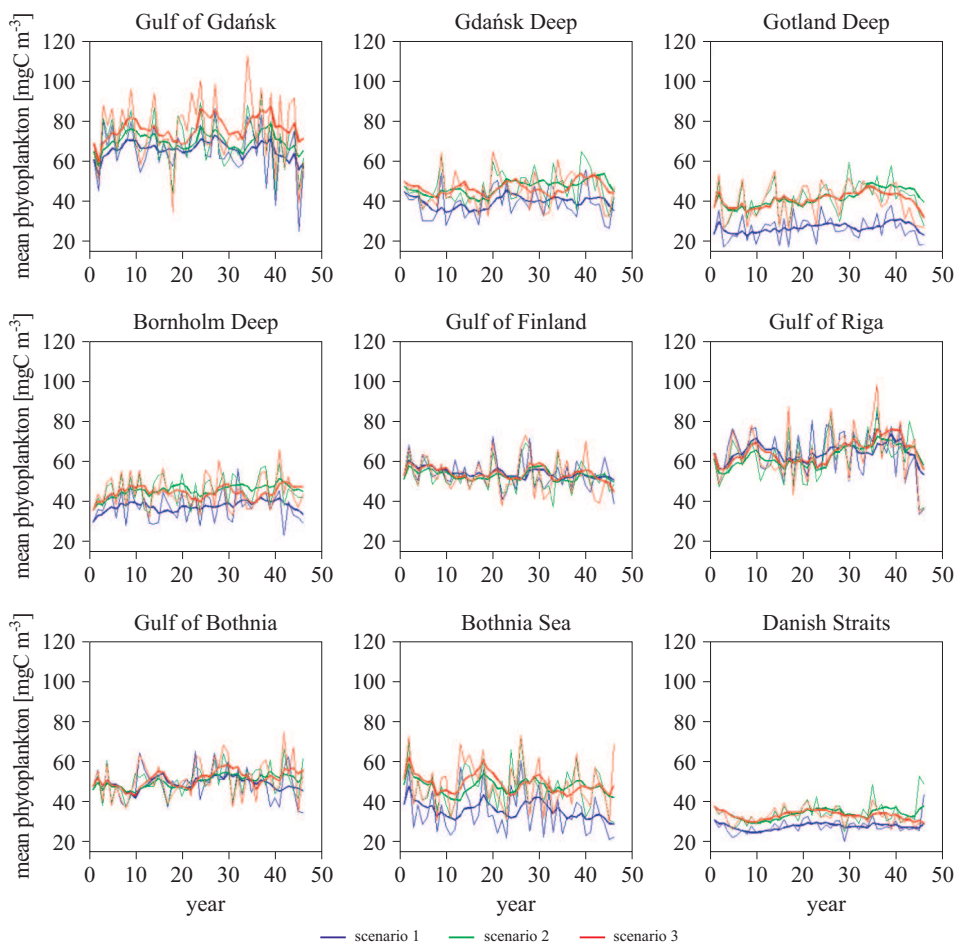
Figure 7. One-year averaged phytoplankton biomass [mgC m^{-3}] of the surface layer at the stations

of the rise in nutrient concentration $Nutr$ in the upper layer caused by the higher wind speed, i.e. by deep mixing. The phytoplankton biomass reflects the availability of nutrients, showing a strong increase with rising total inorganic nitrogen concentration. It shows that increasing wind speed causes currents to exert a greater influence on $Nutr$, which in turn influences $Phyt$ distributions. This is evident in the open sea regions and in the Gulf of Gdańsk, where an increase in current speeds is anticipated.

This increase in primary production and phytoplankton biomass leads to a rise in zooplankton biomass and pelagic detritus concentration. In consequence, there is an increase in the biomass of zooplankton consumed, i.e. by fish. The excess organic matter produced, which sinks to the bottom,
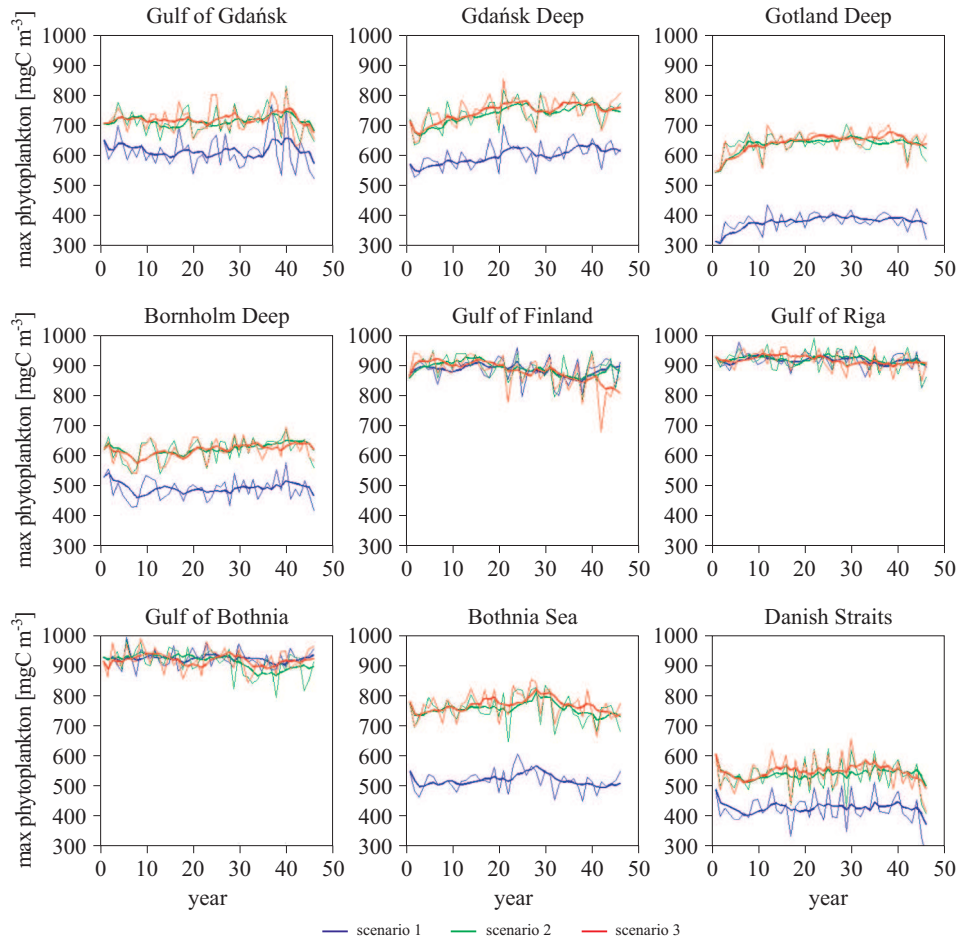
Figure 8. One-year maximum of phytoplankton biomass [mgC m^{-3}] of the surface layer at the stations

is mineralized, leading to anoxia in the near-bottom water. Alternatively, the excess organic matter causes complete oxygen depletion in benthic waters, leading to the production of hydrogen sulphide.

5. Conclusions

Our study demonstrates that ecosystem models have the potential for analysing the distribution and dynamics of primary production. They can also produce a quantitative, regional description and assess variations of organic and inorganic matter in sea water. The temporal resolution produced by the model cannot be achieved by field observations, so the model provides a useful tool for the interpretation of physical and

biogeochemical variables and a valuable complement to field studies. Estimating primary production (phytoplankton biomass) is one of the most important objectives in marine ecology; from this, the amount of energy transferred within communities and ecosystems and supplied to higher trophic levels can be calculated.

The results of the numerical simulations are consistent with in situ observations for temperature and chlorophyll *a* for five years (2000–2004). The differences between the modelled and mean observed phytoplankton biomasses are not small in the subsurface layer; they depend on the month and place for which the calculations were made. They also depend on the C/Chl *a* ratio for converting simulated carbon contents to chlorophyll *a*, which is assumed constant for the whole Baltic.

To reduce the discrepancies between simulated and observed results, future improvements in this model should aspire to include additional state variables for a few groups of phytoplankton assuming the floating C/Chl *a* ratio, including nutrients – not just nitrogen but also phosphate and silicate – as well as zooplankton and pelagic detritus.

The results of numerical simulations of long-term variability in different areas of the Baltic Sea are presented for a period of 45 years. The simulations show a general temporal variation in the distributions investigated. Significant changes in phytoplankton biomass distributions are anticipated, which will take place in regions where current velocities are expected to increase significantly (up to 100 cm s^{-1}). This rise is caused by nutrient concentrations, here driven by wind speed. The calculations also show the influence of short-wave radiation on sea surface temperature.

At present we are developing the 3D Coupled Ecosystem Model of Baltic Sea (for the next version of CEMBS), which consists of three groups of phytoplankton ('diatoms', 'flagellates and others' and 'cyanobacteria'), zooplankton, nutrients (such as PO_4, NO_3, NH_4 and SiO_4) and pelagic detritus for two classes (small and large). The next step in our modelling work will be to increase horizontal and vertical resolution. We also are going to run the ecosystem model (version 2) to study the impact of climate changes on the development of biogeochemical variables in the Baltic Sea.

References

Azam F., Fenchel T., Field J., Gray J. S., Meyer-Reil L. A., Thingstad F., 1982, *The ecological role of water-column microbes in the Sea*, Mar. Ecol. Prog.-Ser., 10, 257–263.

Billen G., Lancelot C., Maybeck M., 1991, *N, P and Si retention along the aquatic continuum from land to ocean*, [in:] *Ocean margin processes in global change*,

R. F. C. Mantoura, J. M. Martin & R. Wollast, Phys. Chem. Earth Sci. Res. Rep., 9, Wiley & Sons, New York, 19–44.

Ciszewski P., 1983, *Estimation of zooplankton biomass and production in the Southern Baltic*, Pol. Ecol. Stud., 9, 387–396.

Dzierzbicka-Głowacka L., 2005, *Modelling the seasonal dynamics of marine plankton in the southern Baltic Sea. Part 1. A Coupled Ecosystem Model*, Oceanologia, 47 (4), 591–619.

Dzierzbicka-Głowacka L., 2006, *Modelling the seasonal dynamics of marine plankton in the southern Baltic Sea. Part 2. Numerical simulations*, Oceanologia, 48 (1), 41–71.

Dzierzbicka-Głowacka L., Kuliński K., Maciejewska A., Jakacki J., Pempkowiak J., 2010a, *Particulate organic carbon in the southern Baltic Sea: numerical simulations and experimental data*, Oceanologia, 52 (4), 621–648.

Dzierzbicka-Głowacka L., Kuliński K., Maciejewska A., Jakacki J., Pempkowiak J., 2011, *Numerical modelling of POC yearly dynamics in the southern Baltic under variable scenarios of nutrients, light and temperature*, Ocean Sci., (submitted).

Dzierzbicka-Głowacka L., Żmijewska I. M., Mudrak S., Jakacki J., Lemieszek A., 2010b, *Population modelling of Acartia spp. in a water column ecosystem model for the South-Eastern Baltic Sea*, Biogeosciences, 7 (7), 2247–2259.

Gordon D. C. Jr., Boudreau P. R., Mann K. H., Ong J.-E., Silvert W. L., Smith S. V., Wattayakorn G., Wulff F., Yanagi T., 1995, *LOICZ biogeochemical modeling guidelines*, LOICZ Rep. Stud., 5, LOICZ Core Proj., Texel, 96 pp.

Jickells T. D., Blackburn T. H., Blanton J. O., Eisma D., Fowler S. W., Mantoura R. F. C., Martens C. S., Moll A., Scharek R., Suzuki Y., Vaulot D., 1991, *What determines the fate of materials within ocean margins?*, [in:] *Ocean margin processes in global change*, R. F. C. Mantoura, J.-M. Martin & R. Wollast (eds.), Dahlem Workshop Rep., 9, Wiley & Sons, Chichester, 211–234.

Mańkowski W., 1978, *Baltic zooplankton and its productivity*, *Productivity of the Baltic Sea ecosystem*, Ossolineum, Wrocław–Warszawa–Kraków–Gdańsk, 113 –134.

Mudrak S., 2004, *Short- and long-term variability of zooplankton in coastal Baltic water using the Gulf of Gdańsk as an example*, Ph. D. thesis, Gdańsk Univ., Gdynia, 323 pp.

Postma H., Rommets J. W., 1984, *Variations of particulate organic carbon in the central North Sea*, Neth. J. Sea Res., 18, 31–50.

Radach G., Moll A., 1993, *Estimation of the variability of production by simulating annual cycles of phytoplankton in the central North Sea*, Progr. Oceanogr., 31 (4), 339–419.

Rozwadowska A., Isemer H.-J., 1998, *Solar radiation fluxes at the surface of the Baltic Proper. Part 1: Mean annual cycle and influencing factors*, Oceanologia, 40 (4), 307–330.

Savchuk O., Wulff F., 1996, *Biogeochemical transformations of nitrogen and phosphorus in the marine environment*, Syst. Ecol. Contrib. No. 2, Stockholm Univ., 79 pp.

Shaffer G., 1987, *Redfield ratios, primary production and organic carbon burial in the Baltic Sea*, Deep-Sea Res., 34, 769–784.

Steele J. H., 1962, *Environment control of photosynthesis in the sea*, Limnol. Oceanogr., 7 (2), 137–150.

Appendix A

Set of CEMBS1 equations with the biochemical processes including parameter values.

$$\frac{\partial Phyt}{\partial t} = -\left(u\frac{\partial Phyt}{\partial x} + v\frac{\partial Phyt}{\partial y}\right) + \frac{\partial}{\partial x}\left(K_x\frac{\partial Phyt}{\partial x}\right) +$$

$$+ \frac{\partial}{\partial y}\left(K_y\frac{\partial Phyt}{\partial y}\right) - (w + w_z)\frac{\partial Phyt}{\partial z} + \frac{\partial}{\partial z}\left(K_z\frac{\partial Phyt}{\partial z}\right) +$$

$$+ PRP - RESP - MORP - GRZ$$

$$\frac{\partial Detr}{\partial t} = D - REMD$$

$$D = \int_0^H [(1 - p_M)MORP + (1 - p_F)FEC + (1 - p_Z)(MORZ +$$

$$+ PRED)]dz$$

$$\frac{\partial Nutr}{\partial t} = -\left(u\frac{\partial Nutr}{\partial x} + v\frac{\partial Nutr}{\partial y}\right) - w\frac{\partial Nutr}{\partial z} +$$

$$+ \frac{\partial}{\partial x}\left(K_x\frac{\partial Nutr}{\partial x}\right) + \frac{\partial}{\partial y}\left(K_y\frac{\partial Nutr}{\partial y}\right) + \frac{\partial}{\partial z}\left(K_z\frac{\partial Nutr}{\partial z}\right) +$$

$$+ g_N[-(PRP - RESP_{\text{light}}) + RESP_{\text{dark}} + p_M MORP + p_F FEC$$

$$+ p_Z(MORZ + PRED) + EXCZ]$$

where u, v, w – the time-dependent velocities obtained from POPCICE, and w_z – sinking velocity of phytoplankton, K_x, K_y, K_z – horizontal and vertical diffusion coefficient (see ECOOP WP 10.1.1).